Catalysis Today 176 (2011) 14–20

Contents lists available at ScienceDirect

Catalysis Today

journal homepage: www.elsevier.com/locate/cattod

Conversion of ethanol over supported cobalt oxide catalysts

P. Rybak*, B. Tomaszewska, A. Machocki, W. Grzegorczyk, A. Denis

The Maria Curie-Sklodowska University, Faculty of Chemistry, Department of Chemical Technology, 3 Maria Curie-Sklodowska Square, 20-031 Lublin, Poland

ARTICLE INFO

Article history:
Received 28 September 2010
Received in revised form 28 February 2011
Accepted 16 June 2011
Available online 14 July 2011

Keywords:
Ethanol
Conversion
Cobalt oxide-based catalysts
Support nature
Deactivation

ABSTRACT

Conversion of ethanol was investigated on supported (ceria, zirconia and ceria–zirconia) cobalt oxide catalysts. The catalysts were prepared by support impregnation with cobalt nitrate–citric acid solution and they were explored by comparing results from different characterization techniques: X-ray fluorescence, X-ray diffraction, Raman spectroscopy and nitrogen adsorption techniques. Their catalytic properties at 693 K were characterized in a fixed-bed reactor. The CoO_x/CeO_2 catalyst displayed the highest catalytic activity. The conversion of ethanol decreased with the increase of the ZrO_2/CeO_2 ratio in the support of catalyst. All catalysts exhibited high selectivity of ethanol conversion to hydrogen and acetone. The coking of catalysts under reaction conditions was also characterized by gravimetric method. The results indicated that the increase of the ZrO_2/CeO_2 ratio in the support exerts significant influence on the coke formation. The amount of carbon deposited on CoO_x/ZrO_2 at 693 K was higher than on any other catalyst. Raman studies of used catalysts proved that their surface was almost completely covered with carbonaceous deposit, which was probably the main reason of deactivation of catalysts under reaction conditions.

1. Introduction

The issues of environmental protection and the growing demand for energy forced people to search for new renewable energy sources. Hydrogen produced from bioethanol in the steam reforming process may become such future fuel. Currently, more than 90% of hydrogen is being produced from natural gas [1–3] or light oil fraction [4]. The use of these unrenewable resources is associated with the emission of greenhouse gases, mainly CO_2, whereas hydrogen produced from ethanol would not only be environmentally friendly but also renewable. Furthermore, ethanol is becoming increasingly available and is free from catalyst poisons such as sulphur compounds [5–9].

A catalyst plays an important role in achieving complete and selective ethanol conversion and is essential for the process to be economically acceptable. In scientific literature there is no strong tendency to use a specific composition of the catalyst that would be most profitable. Various catalytic systems are taken into consideration: transition metals (Ni and Co), noble-metals and bimetallic-based as well as various oxides [5,10–12]. Noble metals (Rh, Ru, Pt, and Pd) supported catalysts are very active in steam reforming of ethanol, but the high cost of these materials limits their application. Cobalt-based catalysts proof to be a much less expensive alternative. Several oxides such as Al_2O_3, MgO, SiO_2, ZrO_2, and ZnO have been used as a cobalt support in steam reforming of ethanol [13–17]. Furthermore, the use of cerium oxide as the support has also been reported. The main advantage of ceria is its oxygen storage capacity and high oxygen mobility associated with oxygen vacancies [18–27]. The insertion of ZrO_2 into Co/CeO_2 structure has been found to enhance the redox properties as well as thermal stability and good anti-carbon deposition ability of these catalysts [28].

Due to the high effectiveness of ceria oxide used as a support and the low cost of cobalt, these materials can form a highly active and selective catalytic system [16,29–37]. However, this system is associated with a major problem which is the deactivation of the catalysts during steam reforming of ethanol due to carbon deposits [31,32,37–40]. In particular Co/CeO_2 was investigated for this reason. Wang et al. [32] studied the deposition of carbon during steam reforming of ethanol over Co/CeO_2. They observed that cobalt particles are completely covered with coke and suggested that this phenomenon was caused by ethylene which played a role of a carbon deposition precursor. The mechanism of Co/ceria catalyst deactivation was studied by de Lima et al. [30]. They suggested that at high temperature acetaldehyde is converted to acetate via support bound –OH. Next, steam promotes decomposition of acetate to carbonate and CH_4, the latter of which decomposes to carbon and H_2. Moreover, in the absence of steam the dehydration to ethylene is favored.

Jilei et al. [41] prepared the catalyst with the use of citric complexes of cerium, zirconium and nickel. They studied the activity of $NiO/Ce_{0.5}Zr_{0.5}O_2$ during the steam reforming process as a function

* Corresponding author at: Uniwersytet Marii Curie-Skłodowskiej, Wydział Chemii, Zakład Technologii Chemicznej, Plac Marii Curie-Skłodowskiej 3, 20-031 Lublin, Poland. Tel.: +48 815375514/815375596; fax: +48 815375565.
E-mail address: rybak-piotr@o2.pl (P. Rybak).

0920-5861/$ – see front matter.
doi:10.1016/j.cattod.2011.06.015

of reaction temperature. They reported that the catalyst prepared by citrate method was more active and selective for hydrogen production at low temperature compared to catalysts prepared by co-precipitation method. In addition, that catalyst demonstrates satisfactory stability, good carbon resistance and anti-sintering properties.

The main results and discussion in the papers listed above were obtained with reduced catalysts, however there are no results concerning unreduced catalysts. The goal of this article was to determine the influence of the nature of the support (ceria, zirconia and ceria–zirconia) and the cerium modifier on the activity and selectivity of unreduced cobalt oxide-based catalysts and on their stability in the ethanol–water conversion.

2. Experimental

The CoO_x/CeO_2, CoO_x/ZrO_2, $CoO_x/Ce_{0.75}Zr_{0.25}O_2$, $CoO_x/Ce_{0.6}Zr_{0.4}O_2$ and CoO_xCeO_2/ZrO_2 catalysts were prepared by the impregnation method. Prior to the impregnation all supports (Aldrich) were dried at 393 K for 3 h. The solutions of cobalt nitrate and citric acid CA (the relative molar concentrations of Co and CA were 1/1) were used for impregnation. In the case of the CoO_xCeO_2/ZrO_2 catalyst the support was impregnated with cobalt and cerium nitrates and citric acid aqueous solution (the Co/Ce and Co + Ce/CA molar ratios were 1/1). After impregnation, the catalyst precursors were dried at 393 K for 12 h, then calcined at 673 K with heating rate of 2.2 K min^{-1} up to the calcination set point and maintained for 1 h at this temperature.

The X-ray fluorescence spectroscopy (XRF) technique was used to determine the bulk contents of cobalt in the catalysts. The spectra of the samples were obtained with the XRF spectrometer (Canberra 1510) equipped with a liquid nitrogen-cooled Si(Li) detector. The AXIL software package for spectra deconvolution and for the calculation of cobalt contents was used.

X-ray diffraction patterns of the catalysts were taken by a Zeiss HZG-4 diffractometer using Mn-filtered CuKα radiation. The samples were scanned by the step-by-step technique, at 2θ intervals of 0.05° and recording time of 10 s for each step. The diffraction data were collected at 20–85°. The Joint Committee on Power Diffraction Standards (JCPDS) database was used for the phase identification.

The Raman spectra were recorded with a resolution of 2 cm^1 in the inVia Raman microscope Renishaw with Raman dispersion system, using a semiconducting laser 785 nm (3 mW), working in a back scattered confocal arrangement. The spectra of all samples were recorded at room temperature.

The Brunauer–Emmett–Teller (BET) surface area of the catalysts was determined by low-temperature (77 K) nitrogen adsorption in the ASAP 2405N v1.0 analyser (Micromeritics). The pore volume and their diameter were evaluated applying the Barrett–Joyner–Halenda (BJH) method.

Temperature-programmed reduction (TPR) experiments were carried out with the Altamira Instruments apparatus equipped with a TCD detector. The reduction profiles were obtained by passing 6% H_2/Ar flow at the rate of 30 mL min^{-1} through 0.05 g of catalyst (0.1–0.2 mm). The temperature was increased from 290 to 800 K at the rate of 10 K min^{-1}. The water vapour that formed during reduction was removed in a cold trap (immersed in a liquid nitrogen–methanol slush) placed before the thermal conductivity detector (TCD).

The reaction of ethanol conversion was carried out at 693 K under atmospheric pressure, in a fixed-bed continuous-flow quartz reactor, using 0.1 g (0.15–0.3 mm) of catalyst diluted (1/10, w/w) with 0.15–0.3 mm grains of quartz. The vapours of ethanol and water were supplied to the reactor with nitrogen as a carrier gas. Molar ratio of $EtOH/H_2O/N_2$ was equalled to 5/20/75. The products of the reaction were analysed with two on-line gas chromatographs. One of them, Varian CP-3800, was equipped with two detectors – a FID and a TCD – as well as two capillary columns: Poropak-Q (for all organics, carbon dioxide and water vapour) and Carbosieve (for methane and carbon monoxide analysis). Helium was used as carrier gas. Hydrogen was analysed by the second gas chromatograph, Chromatron GCHF-18.3, equipped with a charcoal packed column, nitrogen as a carrier gas and a TCD detector.

The total conversion of ethanol X_{EtOH}, conversion of water X_{H_2O} and conversions of ethanol into particular carbon-containing products, X_{CP}, were calculated on the basis of their concentrations before and after the reaction, with a correction introduced for the change in gas volume during the reaction, from the below equations:

$$X_{EtOH} = \frac{C^{in}_{EtOH} - C^{out}_{EtOH}K}{C^{in}_{EtOH}} \times 100\%; \quad X_{H_2O} = \frac{C^{in}_{H_2O} - C^{out}_{H_2O}K}{C^{in}_{H_2O}} \times 100\%;$$

$$X_{CP} = \frac{C^{out}_{CP}K}{(n/2)C^{in}_{EtOH}} \times 100\%$$

where C^{in}_{EtOH} and $C^{in}_{H_2O}$ represent the molar concentrations of ethanol and water in the reaction mixture, mol%; C^{out}_{EtOH} and $C^{out}_{H_2O}$ are the molar concentrations of ethanol and water in the post-reaction mixture, mol%; C^{out}_{CP} is the molar concentration of carbon-containing products in the post-reaction mixture, mol%; n is the number of carbon atoms in the carbon-containing molecule of the reaction product; K is the volume contraction factor ($K = C^{in}_c/C^{out}_c$ where: C^{in}_c and C^{out}_c are the molar concentrations of carbon in ethanol fed to the reaction and in all carbon-containing compounds which were present in post-reaction gases, respectively). The selectivity of ethanol conversion into individual carbon-containing products was expressed as $(X_{CP}/X_{EtOH}) \times 100$. The carbon mass balances, based on the carbon selectivities at each of the reaction temperatures, were close to $100 \pm 3\%$. The selectivity of hydrogen formation was determined from the equation:

$$H_2\text{-selectivity} = \frac{C^{out}_{H_2}}{C^{in}_{H_2} + 2C^{out}_{CH_4} + 2C^{out}_{C_2H_4} + 2C^{out}_{CH_3CHO} + 3C^{out}_{(CH3)_2CO}} \times 100\%$$

where C^{out} refers to the molar concentrations of the hydrogen-containing reaction products, mol%.

The gravimetric method was used to determine the catalyst coking under the ethanol steam reforming conditions. The experiments were conducted in the TG121 microbalance system (Cahn) in a quartz reactor with a continuous flow of ethanol–water vapours. The molar ratio of ethanol and water vapours was 1:4.

3. Results and discussions

Table 1 shows that all catalysts used in the conversion of ethanol had a high surface area 40–60 m^2/g; only $CoO_x/Ce_{0.75}Zr_{0.25}O_2$ was characterized by 120 m^2/g. The catalyst $CoO_x/Ce_{0.75}Zr_{0.25}O_2$ exhibited the highest porosity. The pore diameter of that catalyst was 7.7 nm and the pores volume – 0.284 cm^3/g. In the case of the CoO_x/CeO_2 catalyst the pore diameter was similar and amounted to 8.8 nm. It can be noticed that the higher content of zirconia in the support, the larger pore diameter could be expected. In the case of $CoO_x/Ce_{0.6}Zr_{0.4}O_2$ the pore size was 10.7 nm and it increased to 19.1 nm for CoO_x/ZrO_2. The cobalt content was in the range of 8–10 wt.%.

Fig. 1A shows XRD patterns of cobalt and cobalt–cerium supported catalysts. Ceria and ceria–zirconia (with high cerium

Table 1
Results of characterization of cobalt oxide-based catalysts.

Catalysts	BET surface area (m^2/g)	Average diameter of pores (nm)	Volume of pores (cm^3/g)	Cobalt (wt.%)
CoO_x/CeO_2	66.9	8.8	0.1907	7.89 ± 0.32
$CoO_x/Ce_{0.75}Zr_{0.25}O_2$	118.2	7.7	0.2840	9.61 ± 0.38
$CoO_x/Ce_{0.6}Zr_{0.4}O_2$	56.0	10.7	0.1923	8.59 ± 0.34
CoO_x/ZrO_2	40.5	19.1	0.2411	8.19 ± 0.33
CeO_xCoO_x/ZrO_2	63.5	9.4	0.1748	9.07 ± 0.36

content) supports enabled us to obtain a very high dispersion of the cobalt oxide phase. Similar effect was achieved when cobalt was deposited simultaneously with cerium from the same solution on the zirconia support (the case of the CoO_xCeO_2/ZrO_2 catalyst). Neither Co_3O_4 nor Co_2O_3 or CoO peaks could be seen in the XRD patterns for ceria-contained supported cobalt catalysts. The absence of the peaks of cobalt oxides proves their very small crystallite size. Only in the case of CoO_x/ZrO_2, it was possible to determine the cobalt oxide crystallite size, which was 9.2 nm. The XRD study also revealed the presence of a new phase, which we have not identified yet.

Fig. 1B displays the Raman spectra of the catalysts. They reveal five bands in the range of 100–1200 cm^{-1}. The signals located at approximately 196, 484, 522, 622, and 693 cm^{-1} correspond to the F_{2g}, E_g, F_{2g}, F_{2g}, and A_{1g} modes, respectively, of the crystalline Co_3O_4 phase [42–44]. It is known that the Raman spectrum for pure ceria displays only one peak at 465 cm^{-1}, as expected on the basis of the factor group analysis and in agreement with the literature [45–55]. This peak corresponds to the triply degenerate F_{2g} mode of fluorite CeO_2. Furthermore, the pure zirconium oxide exhibits peaks at 182 (A_g), 333 (B_g), 377 (B_g), 475 (A_g), 559 (A_g), and 634 cm^{-1} (A_g) characteristic for monoclinic ZrO_2 [56–58] and six Raman bands at 145 (B_{1g}), 265 (E_g), 313 (B_{1g}), 460 (E_g), 600 (B_{1g}) and 645 cm^{-1} (E_g) predicted theoretically for tetragonal ZrO_2 [48,51–55,59,60,57,61]. It can be observed in the Raman spectra of our catalysts that, except for the ceria supported CoO_x/CeO_2 catalyst, there are no signals derived from any of the support. Only a small peak of ceria is visible at 465 cm^{-1}. Additionally, there occurs no masking effect associated with cobalt oxide. The presence of only very strong Raman signals of Co_3O_4 suggests that the surface of the catalysts is completely covered with crystallites of Co_3O_4.

The temperature-programmed reduction profiles (Fig. 2) for all catalysts were complex and difficult to interpret unambiguously. They show two groups of peaks: the low-temperature group (in the range of 423–573 K) attributed to the reduction of Co_3O_4 to CoO and then to metallic cobalt and the second group in the range of 573–673 K [28,33]. The reduction of some amounts of cobalt oxides in all catalysts was very hard. Those more difficult reducible cobalt oxide forms are most probably strongly interacting with the support (e.g., as a solid solution). Liu et al. [62] studied the soot catalytic combustion over the nanometric CeO_2-supported cobalt oxide catalysts prepared by means of ultrasonic-assisted incipient-wetness impregnation. They reported that the structures of the catalyst were altered with the loading amount of cobalt. At low Co loading, cobalt oxide existed as CoO or Co–Ce–O solid solution, and the medium or high Co loading resulted in the presence of Co_3O_4 spinel. The existence of a strong interaction between cobalt oxide species and the mesoporous support CeO_2 was also concluded by Dongsheng et al. [63]. They studied CO and CH_4 catalytic oxidation over CeO_2–MO_x (M = Cu, Mn, Fe, Co, and Ni) prepared by a citric acid complexation–combustion method. Their XRD and Raman results confirmed presence of the solid solutions between CeO_2 and Co_3O_4. As reported in the literature, ceria is characterized by a low-temperature peak and high-temperature peak of reduction with hydrogen [64,65]. In the case of our ceria-containing catalysts the reduction of ceria is seen only in the case of CoO_x/CeO_2 above 973 K.

de la Piscina et al. [66] studied the steam reforming of ethanol over cerium oxide. They carried out the process between 573 and 723 K, at atmospheric pressure, using a 1:13:70 C_2H_5OH:H_2O:Ar stream (molar ratio). The conversion of ethanol increased with temperature and at 723 K, it reached the value of 24%. The main products obtained after 20 h of reaction were hydrogen, ethylene,

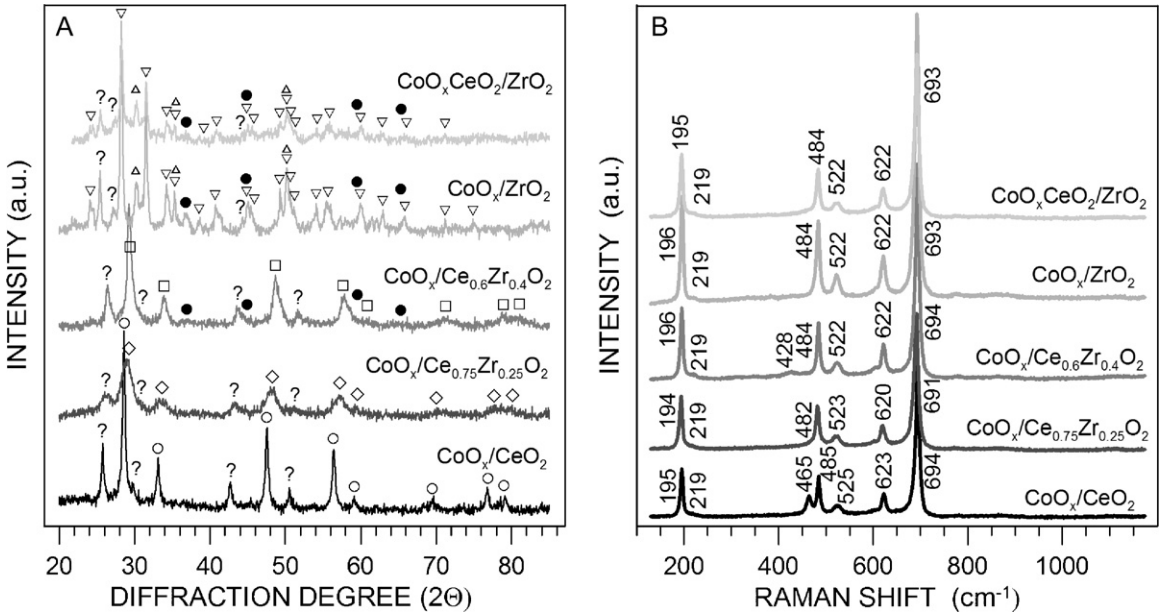

Fig. 1. (A) XRD patterns of ceria-, ceria–zirconia- and zirconia-supported cobalt oxide and cobalt oxide–cerium oxide catalysts: ○, CeO_2; ◊, $Ce_{0.75}Zr_{0.25}O_2$; □, $Ce_{0.6}Zr_{0.4}O_2$; △, ▽ ZrO_2; ●, Co_3O_4; ?, unknown phase; (B) Raman spectra of ceria-, ceria–zirconia- and zirconia-supported cobalt oxide and cobalt oxide–cerium oxide catalysts.

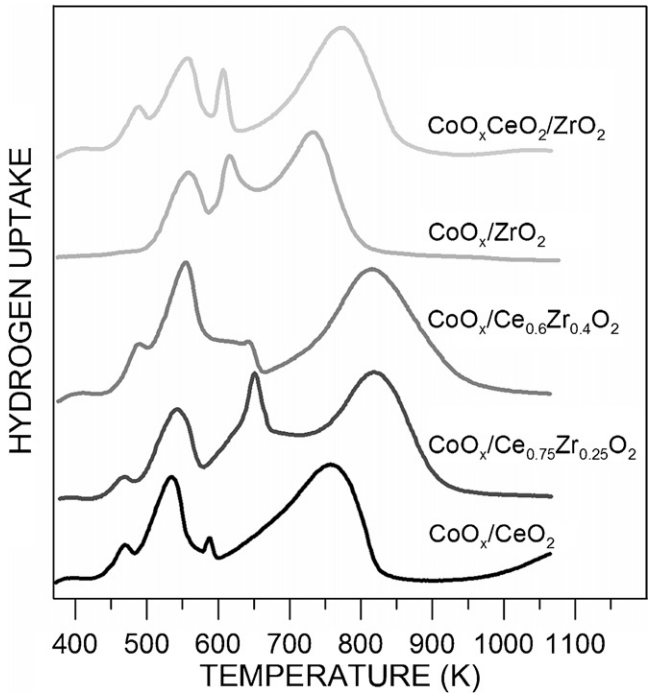

Fig. 2. TPR profiles of ceria-, ceria–zirconia- and zirconia-supported cobalt oxide and cobalt oxide–cerium oxide catalysts.

carbon dioxide and acetone. Also de Lima et al. [67] studied the steam reforming of ethanol over $CeZrO_2$ (Ce/Zr ratio = 3.0) at 773 K (residence time = 0.02 g s/mL). They concluded that the ethanol conversion was nearly 70% on $CeZrO_2$ and it was quite stable during 6 h (H_2O/ethanol molar ratio 5.0). The product distributions exhibited mainly formation of ethylene and hydrogen. Trace amounts of carbon dioxide, methane and acetaldehyde were also detected, while the formation of CO was not observed. These researches suggested that cerium oxide shows small activity in the steam reforming of ethanol. The coupling of cerium oxide and zirconium oxide forms an active catalytic system but this system mainly exhibits the formation of ethylene (a strong coke precursor).

The catalytic behaviour of our catalysts in the ethanol steam reforming conditions is presented in Fig. 3 in terms of ethanol and water conversions and selectivities versus reaction time. The initial activity of catalysts formed the following order: $CoO_x/CeO_2 \approx CoO_x/Ce_{0.75}Zr_{0.25}O_2 > CoO_x/Ce_{0.6}Zr_{0.4}O_2 > CoO_xCeO_2/ZrO_2 > CoO_x/ZrO_2$. The content of zirconium oxide in the catalyst support had a significant effect on the conversion of ethanol and water. The conversion of ethanol decreased parallel to the increase of the ZrO_2/CeO_2 ratio. In terms of stability of catalytic properties, all catalysts deactivated with time on stream under reaction conditions and the ethanol conversion decreased considerably within a few hours. Among the tested catalysts, CoO_x/CeO_2 and $CoO_x/Ce_{0.75}Zr_{0.25}O_2$ displayed the highest stability. Over the CoO_x/CeO_2 catalyst, the initial conversion of ethanol was 70% and it decreased after 20 h of reaction to 60% at 693 K. In the case of the most unstable catalyst, $CoO_x/Ce_{0.6}Zr_{0.4}O_2$, the conversion of ethanol decreased from 60% to 20% after 20 h, most probably due to intensive coking and/or sintering of the catalyst. Over oxide form of cobalt catalysts, the steam reforming of ethanol occurs only to the limited extent, which is suggested by low water conversion.

The influence of the nature of the support had no significant impact on the selectivity of ethanol conversion to the most desirable products – hydrogen and carbon dioxide (Fig. 3). They were in the range of 56–64% and 18–25%, respectively. The CoO_x/CeO_2 displayed the highest selectivity of ethanol conversion to CO_2 (25%). In the case of $CoO_x/Ce_{0.75}Zr_{0.25}O_2$ and $CoO_x/Ce_{0.6}Zr_{0.4}O_2$ catalysts this selectivity was very similar. The lowest selectivity, below 20%, was for CoO_x/ZrO_2. Acetone, acetaldehyde and small amounts of other organic by-products, as well as traces of carbon monoxide were also formed in side reactions. In particular, the selectivity towards acetone appeared exceptionally high, initially even above 60%. The presence of cerium oxide in the support favored high selectivity of acetone formation. That direction of ethanol conversion was less significant for the CoO_x/ZrO_2 catalyst.

The presence of CeO_2 in the cobalt oxide phase can be considered a valuable modification of this phase in the zirconia supported catalyst. It resulted in the CoO_xCeO_2/ZrO_2 catalyst being characterized by smaller cobalt oxide crystallite size (no signal in the X-ray diffraction pattern) and by higher BET surface area (63.5 m^2/g) than in the case of the CoO_x/ZrO_2. The pore diameter was 9.4 nm and it was lower in comparison with CoO_x/ZrO_2 (Table 1). Those positive facts also caused a change in the activity of the catalyst (Fig. 2). The selectivity of the ethanol conversion to hydrogen and carbon dioxide increased by 10%, parallel to the decrease of selectivity towards acetaldehyde, ethylene and methane with respect to CoO_x/ZrO_2 (Fig. 3).

The stability of activity and selectivity is an important characteristic of any catalyst since it determines its efficient use in a reaction. A decrease in stability of catalysts may be attributed to the deposition of coke and sintering of the active phase. Ethylene is known as a strong coke precursor and carbon formation appeared primarily due to its presence in the product stream. It should be noted that the selectivity of ethylene formation is inversely proportional to the activity of catalysts and the quickness of their deactivation which can be observed. This relation is most probably connected with carbonaceous deposits formation [30–32]. The weight of coke or carbon deposited on catalysts during ethanol conversion was obtained from TG results (Fig. 4A). At first, the catalysts were heated to constant weight at 623 K. Then the catalysts were treated in the stream of ethanol and water vapours (molar ratio H_2O/EtOH = 4:1) and heated to 693 K. It can be observed that TG profiles are a product of two phenomena: the reduction of catalysts and carbon deposition at 693 K. The rate and amount of carbon deposited on CoO_x/ZrO_2 were significantly higher than on any other catalyst. Moreover, initial conversion of ethanol was the lowest on this catalyst (Fig. 3). Relatively large amounts of coke were also deposited over $CoO_x/Ce_{0.6}Zr_{0.4}O_2$, but with much lower rate than in the case of the CoO_x/ZrO_2 catalyst. Ethanol conversion decreased very quickly on that catalyst (Fig. 3). The formation of coke deposits was also confirmed by the Raman spectroscopy of used catalysts after the ethanol conversion. Fig. 4B shows the Raman spectra taken over CoO_x/CeO_2, CoO_x/ZrO_2 and CoO_xCeO_2/ZrO_2 after 25 h on the steam reforming at 693 K. Two bands are observed around 1312 cm^{-1} and 1599 cm^{-1} and these signals are characteristic of disordered carbonaceous and ordered graphitic species [68,23]. No bands of cobalt oxide or support oxides were seen. Those results revealed that the surface of catalysts was completely covered by coke. We may conclude that the coke formation and encapsulation of catalyst particles are justified reasons of deactivation of catalysts in the ethanol conversion reaction.

Song and Ozkan [23] have conducted research on Co/ZrO_2 catalysts in the steam reforming of ethanol. They obtained a complete conversion of ethanol at 400 °C (EtOH:H_2O = 1:10 (molar ratio)), while that catalyst deactivated rapidly due to carbon deposition on the surface. Addition of 10% CeO_2 to the support maintained its stable activity and also imparted higher reforming activity to the catalyst. The main products obtained after 25 h of reaction were hydrogen and carbon dioxide on $Co/10\%CeO_2$–ZrO_2. Also Zhang et al. [33] studied the steam reforming of ethanol over Co/CeO_2. They concluded that the ethanol conversion was complete on this catalyst at 400 °C (EtOH/H_2O/He = 2/18/80 vol%) and it was quite

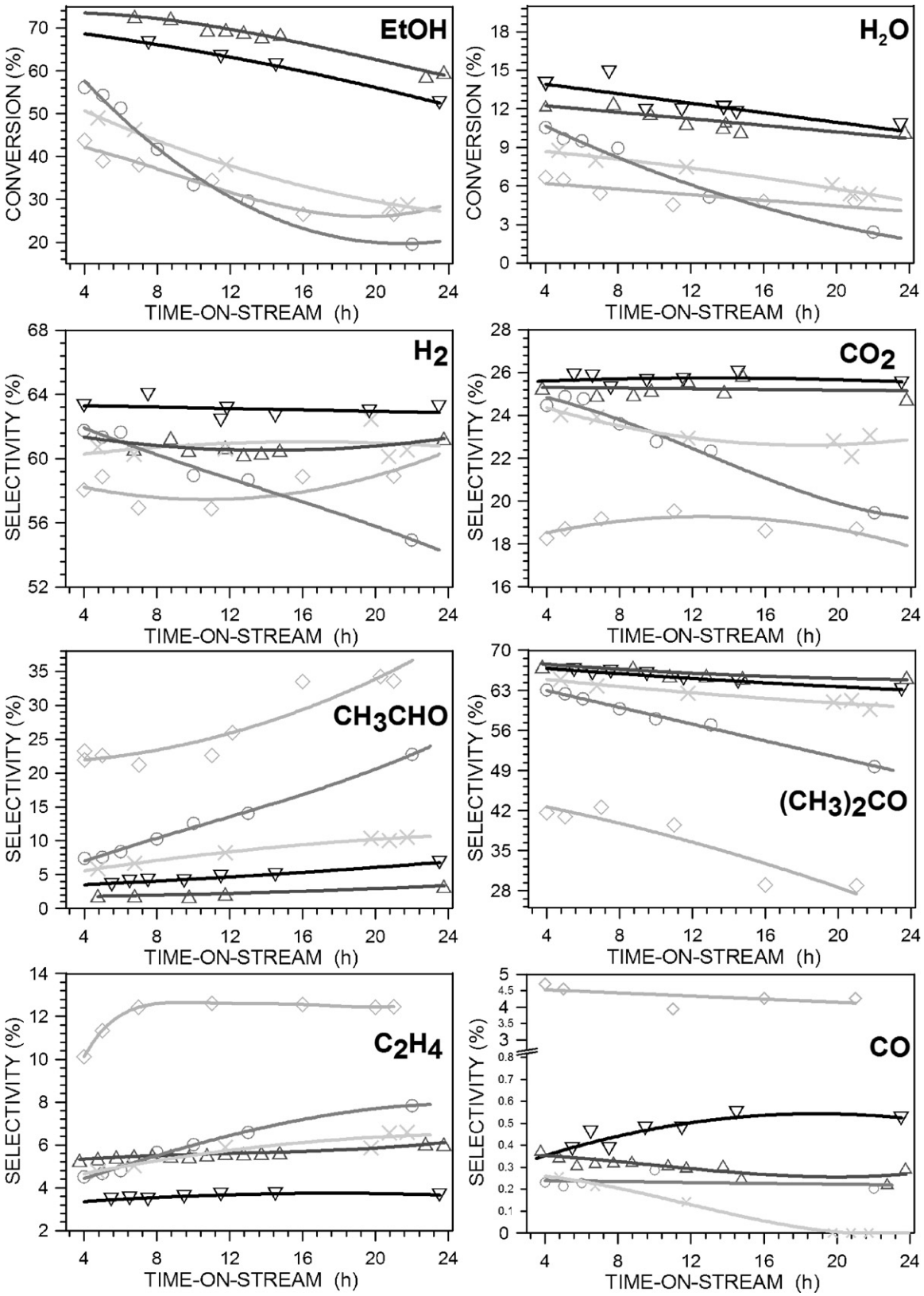

Fig. 3. Conversion of ethanol and water and selectivity to the reaction products over supported cobalt oxide-based catalysts (693 K, EtOH/H_2O/N_2 = 5/20/75 mol/mol/mol): ▽, CoO_x/CeO_2; △, $CoO_x/Ce_{0.75}Zr_{0.25}O_2$; ○, $CoO_x/Ce_{0.6}Zr_{0.4}O_2$; ◊, CoO_x/ZrO_2; ×, CoO_xCeO_2/ZrO_2.

stable. The product distribution exhibited mainly the formation of hydrogen and carbon dioxide, which was constant during the reaction. Slight amounts of methane and acetaldehyde were also detected. The main results and discussions in the above mentioned papers were obtained over reduced catalysts and for this reason they are not easily comparable with our results. Our studies of unreduced cobalt oxide-based catalysts showed that there is a possibility to obtain not only hydrogen but also acetone. We also

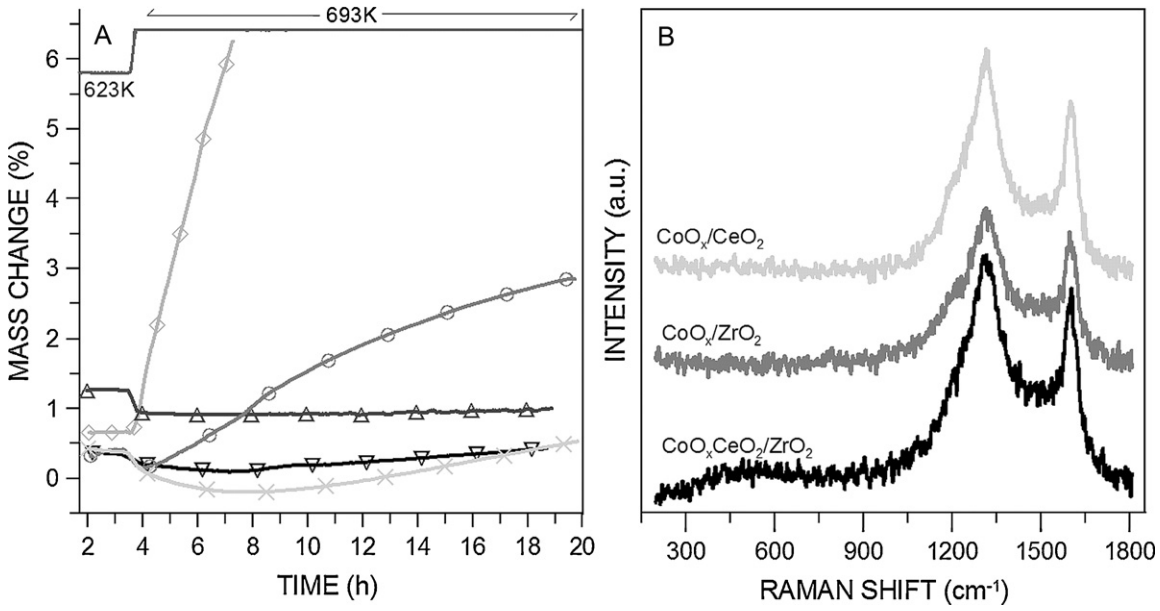

Fig. 4. (A) Thermogravimetric profiles of ▽, CoO_x/CeO_2; △, $CoO_x/Ce_{0.75}Zr_{0.25}O_2$; ○, $CoO_x/Ce_{0.6}Zr_{0.4}O_2$; ◊, CoO_x/ZrO_2; ×, CoO_xCeO_2/ZrO_2 under reaction conditions (the molar ratio of ethanol and water vapours was 1:4); (B) Raman spectra of ceria- and zirconia-supported cobalt oxide and cobalt oxide–cerium oxide catalysts after the ethanol–water reaction.

obtained the improvement of stability of zirconia supported cobalt catalysts by addition of cerium into the cobalt phase. Moreover, the clear relation between the amount of ceria in the support and the stability of catalysts could be observed. The more ceria oxide was in the support, the higher stability had the catalyst.

4. Conclusions

It was shown that there is a possibility to obtain not only hydrogen but also acetone over unreduced cobalt oxide-based catalysts from bio-ethanol. The conversion of ethanol and its selectivity are strongly influenced by the nature of the support. The CoO_x/CeO_2 and $CoO_x/Ce_{0.75}Zr_{0.25}O_2$ catalysts enabled us to achieve the highest and most stable activity measured in the conversion of ethanol, whereas the presence of higher amounts of zirconium oxide in the support resulted in a decrease in conversion and the CoO_x/ZrO_2 catalyst was the least active. An improvement of the catalytic properties of the latter catalyst is possible by modifying its active phase with cerium. However, all catalysts demonstrated some instability of their activity, which was directly proportional to the amount of zirconia in the catalyst support. The most significant reason for the diminishing stability was most probably the coke deposition. Its formation seems to be connected with the polymerization of ethylene on the catalyst surface.

Acknowledgements

These results have been achieved within the framework of the 1st call on Applied Catalysis carried out by ACENET ERA-NET (project ACE.07.009), with funding from the Ministry of Science and Higher Education of Poland.

References

[1] J.R. Rostrup-Nielsen, Catal. Rev. 46 (2004) 247.
[2] J.N. Armor, Appl. Catal. A: Gen. 176 (1999) 159.
[3] J.D. Holladay, Y. Wang, E. Jones, Chem. Rev. 104 (2004) 4767.
[4] P. Ferreira-Apariciao, M.J. Benito, Catal. Rev. 47 (2005) 491.
[5] A. Haryanto, S. Fernando, N. Murali, S. Adhikari, Energy Fuels 19 (2005) 2098.
[6] F. Mariño, M. Boveri, G. Baronetti, M. Laborde, Int. J. Hydrogen Energy 29 (2004) 67.
[7] G.A. Deluga, J.R. Salge, L.D. Schmidt, X.E. Verykios, Science 303 (2004) 993.
[8] S. Fernando, M. Hanna, Energy Fuels 18 (2004) 1695.
[9] K. Vasudeva, N. Mitra, P. Umasankar, S.C. Dhingra, Int. J. Hydrogen Energy 21 (1996) 13.
[10] P. Vaidya, A.E. Rodriugues, Chem. Eng. 117 (2006) 39.
[11] M. Ni, D.Y.C. Leung, M.K.H. Leung, Int. J. Hydrogen Energy 32 (2007) 3238.
[12] P.K. Cheekatamarla, C.M. Finnerty, J. Power Sources 160 (2006) 490.
[13] M.S. Batista, R.K.S. Santos, E.M. Assaf, J.M. Assaf, E.A. Ticianelli, J. Power Sources 124 (2003) 99.
[14] A. Kaddouri, C. Mazzocchia, Catal. Commun. 5 (2004) 339.
[15] J. Llorca, N. Homs, J. Sales, P.R. de la Piscina, J. Catal. 209 (2002) 306.
[16] H. Wang, J.L. Ye, Y. Liu, Y.D. Li, Y.N. Qin, Catal. Today 129 (2007) 305.
[17] F. Haga, T. Nakajima, H. Miya, S. Mishima, Catal. Lett. 48 (1997) 223.
[18] S.M. de Lima, I.O. da Cruz, G. Jacobs, B.H. Davis, L.V. Mattos, F.B. Noronha, J. Catal. 257 (2008) 356.
[19] W. Cai, F. Wanga, E. Zhan, A.C. Van Veen, C. Mirodatos, W. Shen, J. Catal. 257 (2008) 96.
[20] J. Kugai, V. Subramani, C. Song, M.H. Engelhard, Y.H. Chin, J. Catal. 238 (2006) 430.
[21] H. Roh, A. Platon, Y. Wang, D.L. King, Catal. Lett. 110 (2006) 1.
[22] C.E. Hori, H. Permana, K.Y.S. Ng, A. Brenner, K. More, K.M. Rahmoeller, D. Belton, Appl. Catal. B: Environ. 16 (1998) 105.
[23] H. Song, U.S. Ozkan, J. Catal. 261 (2009) 66.
[24] R.J. Gorte, S. Zhao, Catal. Today 104 (2005) 18.
[25] S. Rossignol, F. Gerard, D. Duprez, J. Mater. Chem. 9 (1999) 1615.
[26] A. Trovarelli, F. Zamar, J. Llorca, C. de Leitenburg, G. Dolcetti, J.T. Kiss, J. Catal. 169 (1997) 490.
[27] H.-S. Roh, H.S. Potdar, K.-W. Jun, Catal. Today 93–95 (2004) 39.
[28] B. Zhang, X. Tang, Y. Li, W. Cai, Y. Xu, W. Shen, Catal. Commun. 7 (2006) 367.
[29] S.S.-Y. Lin, H. Daimon, S.Y. Ha, Appl. Catal. A: Gen. 366 (2009) 252.
[30] S.M. de Lima, A.M. da Silva, L.O.O. Da Costa, U.M. Graham, G. Jacobs, B.H. Davis, L.V. Mattos, F.B. Noronha, J. Catal. 268 (2009) 268.
[31] J.C. Vargas, S. Libs, A.C. Roger, A. Kiennemann, Catal. Today 107 (2005) 417.
[32] H. Wang, Y. Liu, L. Wang, Y.N. Qin, Chem. Eng. J. 145 (2008) 25.
[33] B. Zhang, X. Tang, Y. Li, W. Cai, Y. Xu, W. Shen, Int. J. Hydrogen Energy 32 (2007) 2367.
[34] M. Benito, R. Padilla, L. Rodriguez, J.L. Sanz, L. Daza, J. Power Sources 169 (2007) 167.
[35] H. Song, L.Z. hang, R.B. Watson, D. Braden, U.S. Ozkan, Catal. Today 129 (2007) 346.
[36] L.F. Liotta, G.D. Carlo, G. Pantaleo, G. Deganello, Catal. Commun. 6 (2005) 329.
[37] A.M. da Silva, L.O.O. Da Costa, K.R. Souza, L.V. Mattos, F.B. Noronha, Catal. Commun. 11 (2010) 736.
[38] F. Romero-Sarria, J.C. Vargas, A. Roger, A. Kiennemann, Catal. Today 133 (2008) 149.
[39] J.M. Guil, N. Homs, J. Llorca, P.R. de la Piscina, J. Phys. Chem. B 109 (2005) 10813.
[40] A.E. Galetti, M.F. Gomez, L.A. Arrua, A.J. Marchi, M.C. Abello, Catal. Commun. 9 (2008) 1201.
[41] Y. Jilei, W. Yang, L. Yuan, J. Rare Earths 26 (2008) 831.
[42] V.G. Hadjiev, M.N. Iliev, I.V. Vergilov, J. Phys. C: Solid State Phys. 21 (1988) 199.
[43] X.-P. Shen, H.-J. Miao, H.Z.Z. Xu, Appl. Phys. A 9 (2008) 47.

[44] V.G. Hadjiev, M.N. Lliev, J.V. Verilov, J. Phys. C: Solid State Phys. 21 (1988) 199.
[45] W.H. Weber, K.C. Hass, J.R. McBride, Phys. Rev. B 48 (1993) 178.
[46] S. Kanakaraju, S. Mohan, A.K. Sood, Thin Solid Films 305 (1997) 191.
[47] S. Wang, W. Wang, J. Zuo, Y. Qian, Mater. Chem. Phys. 68 (2001) 246.
[48] V.S. Escribano, E.F. López, M. Panizza, C. Resini, J.M.G. Amores, G. Busca, Solid State Sci. 5 (2003) 1369.
[49] A. Martínez-Arias, D. Gamarra, M. Fernández-García, X.Q. Wang, J.C. Hanson, J.A. Rodriguez, J. Catal. 240 (2006) 1.
[50] D. Terribile, A. Trovarelli, J. Llorca, C. de Leitenburg, G. Dolcetti, Catal. Today 43 (1998) 79.
[51] J. Kaspar, P. Fornasiero, G. Balducci, R. Di Monte, N. Hickey, V. Sergo, Inorg. Chim. Acta 349 (2003) 217.
[52] J.-R. Kim, W.-J. Myeong, S.-K. Ihma, J. Catal. 263 (2009) 123.
[53] R. Si, Y.-W. Zhang, S.-J. Li, B.-X. Lin, C.-H. Yan, J. Phys. Chem. B 108 (2004) 12481.
[54] X. Wu, X. Wu, Q. Liang, J. Fan, D. Weng, Z. Xie, S. Wei, Solid State Sci. 9 (2007) 636.
[55] T. Hirata, J. Phys. Chem. Solids 56 (1995) 951.
[56] C. Schild, A. Wokaun, R.A. Koeppel, A. Baiker, J. Catal. 130 (1991) 657.
[57] M. Li, Z. Feng, G. Xiong, P. Ying, Q. Xin, C. Li, J. Phys. Chem. B 105 (2001) 8107.
[58] K.A. Pokrovski, M.D. Rhodes, A.T. Bell, J. Catal. 235 (2005) 368.
[59] E. Fernández López, V. Sánchez Escribano, M. Panizza, M.M. Carnasciali, G. Busca, J. Mater. Chem. 11 (2001) 1891.
[60] T. Hirata, E. Asari, M. Kitajima, J. Solid State Chem. 110 (1994) 201.
[61] G. Águila, F. Gracia, P. Araya, Appl. Catal. A: Gen. 343 (2008) 16.
[62] J. Liu, Z. Zhao, J. Wang, Ch. Xu, A. Duan, G. Jiang, Q. Yang, Appl. Catal. B: Environ. 84 (2008) 185–195.
[63] Q. Dongsheng, L. Guanzhong, G. Yun, W. Yanqin, G. Yanglong, J. Rare Earths 28 (2010) 742.
[64] J. Kaspar, P. Fornasiero, M. Graziani, Catal. Today 50 (1999) 285.
[65] D. Terribile, A. Trovarelli, J. Llorca, C. de Leitenburg, A. Primavera, G. Dolcetti, Catal. Today 47 (1999) 133.
[66] J. Llorca, P.R. de la Piscina, J. Sales, N. Homs, Chem. Commun. 7 (2001) 641.
[67] S.M. de Lima, A.M. Silva, U.M. Graham, G. Jacobs, B.H. Davis, L.V. Mattos, F.B. Noronha, Appl. Catal. A: Gen. 352 (2009) 95.
[68] J. Llorca, N. Homs, J. Sales, J.L.G. Fierro, P.R. de la Piscina, J. Catal. 222 (2004) 470.